

# Ultrasonic oscillator driver with digital frequency sweep function

Chung-Wen Hung, Yu-Hsing Su, Chun-Chieh Wang

National Yunlin University of Science and Technology, Taiwan

123 University Road, Section 3, Douliou, Yunlin 64002, Taiwan, R.O.C

Email: wenhung@yuntech.edu.tw, M11212048@yuntech.edu.tw, jasonccw@yuntech.edu.tw

## Abstract

An Ultrasonic oscillator driver with digital frequency sweep function is proposed in this paper. Ultrasonic transducers are widely utilized in various applications, such as liquid atomization. The drive circuit causes the ultrasonic transducer to vibrate, while the attached atomization component converts the liquid into fine particles. In this paper, the LC resonant circuit is adopted to drive the ultrasonic transducer. Due to small variations in the resonant frequency of each transducer, the optimal operating frequency also varies and may change as physical conditions change. Then, microcontroller units (MCU) are used to control circuit switches to achieve frequency adjustment, scanning and tracking, so that the ultrasonic oscillator works in the best state.

*Keywords:* Ultrasonic Transducer, Frequency Scanning, Frequency Tracking

## 1. Introduction

Ultrasonic waves, which originated in the 19th century, are sound waves with frequencies exceeding 20 kHz. In recent years, the applications of ultrasonic waves have expanded significantly, encompassing medical tools such as ultrasonic scalpels [1] and industrial processes like ultrasonic cleaning and welding [2]. Common piezoelectric materials include Zinc Oxide (ZnO), Polyvinylidene Fluoride (PVDF), and Lead Zirconate Titanate (PZT). Among these, PZT is favored due to its higher piezoelectric coefficient, making it widely utilized in various applications. Ultrasonic transducers are constructed using PZT piezoelectric materials [3]. However, the resonance frequency of these materials can fluctuate due to changes in mechanical structure, component aging, and temperature increases resulting from prolonged operation [4], [5], [6]. To address this issue, this paper proposes an automatic frequency-tracking approach that periodically adjusts the transducer's frequency, ensuring it returns to the optimal oscillation point even after frequency drift, thereby maintaining adequate vibration output.

## 2. Load and System Architecture

### 2.1. Ultrasonic Transducer Architecture

The ultrasonic transducer selected for this study is a 50W, 28kHz bolt-clamped Langevin transducer (BLT) for testing purposes. This transducer is known for its high conversion efficiency and allows for selecting different operating frequencies based on specific applications [7].

This study analyzes the variation in impedance phase within the transducer by conducting a frequency sweep using an LCR meter. As shown in Fig. 1, the sweep results for a 28 kHz ultrasonic transducer reveal a

resonance frequency of 28.06 kHz with an impedance of 29  $\Omega$ . To achieve sufficient vibration for atomizing water, an amplitude horn is added, as illustrated in Fig. 2. The horn focuses the vibrations at a single point to produce a greater vibrational output. The sweep results after adding the horn are presented in Fig. 3, where the overall impedance phase differs significantly, and the resonance frequency shifts to 27.22 kHz with an impedance of 49  $\Omega$ . The transducer equipped with the amplitude horn will be used as the test component in this study.

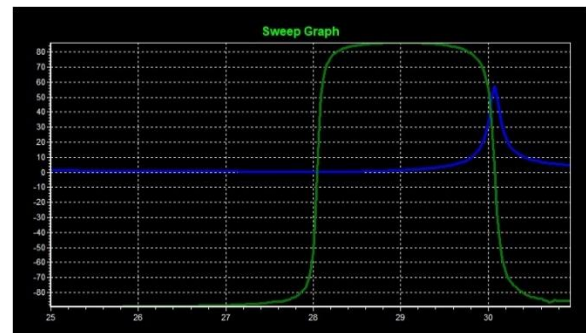


Fig. 1 Impedance Phase Plot of an Unloaded 28 kHz Transducer



Fig. 2 Schematic diagram of transducer with amplitude horn

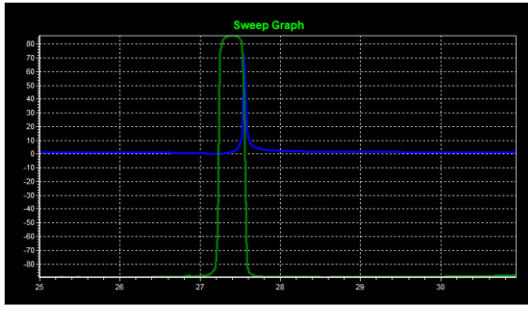


Fig. 3 Impedance phase plot of a 28kHz transducer with amplitude horn

2.2. Hardware Architecture

The hardware architecture of this study is illustrated in Fig. 4 The primary power source utilizes a power supply for voltage adjustment, enabling fine-tuning based on various oscillation effects. A half-bridge inverter with LC resonance functions as the main driving circuit, converting DC power into high-frequency AC at the desired frequency. The LC resonance effectively filters out higher harmonics, producing a sine wave for the transducer. The LC resonance frequency is calculated using Equation (1), where the LC components are optimized to achieve the best resonance. For the auxiliary power supply, a 25V input is converted to 18V and 3.3V using a buck converter to power the driver and the MCU, respectively. To monitor the transducer’s current state, a current transformer (CT) is employed to detect current feedback to the MCU.

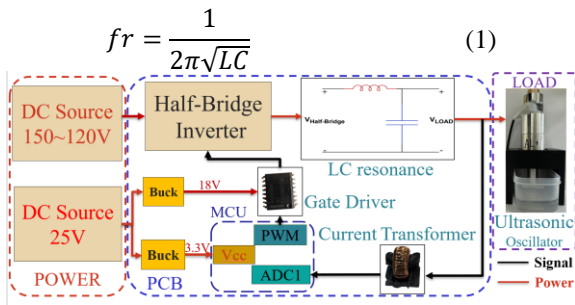


Fig. 4 Hardware Architecture Diagram

2.3. Software Flowchart

The resonant frequency range of the loaded transducer is approximately between 27 kHz and 27.5 kHz. As a capacitive component, the transducer exhibits slight frequency variations that may drift due to factors such as temperature fluctuations and long-term usage deterioration. In this study, a microcontroller unit (MCU) performs digital frequency sweeping and periodically monitors the frequency after each sweep. Fig. 5 illustrates the frequency-tracking flowchart: after identifying the operating frequency within the sweep range, a sweep of

±0.5 kHz around the current operating frequency is conducted every 3 minutes. The frequency with the highest current in this range is selected as the new operating frequency. The interval is set at 3 minutes to prevent excessive tracking, which could lead to rapid temperature increases in the transducer and result in adverse effects.

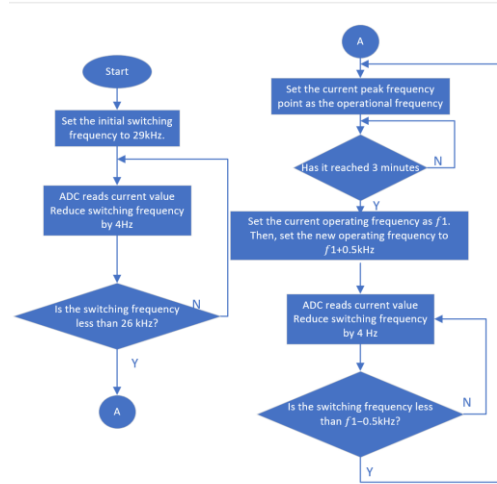


Fig. 5 Frequency Tracking Flowchart

3. Results and Discussion

In this study, an actual circuit is employed with a frequency-tracking method to drive the transducer, recording changes in temperature and transducer power over time to validate the feasibility of the tracking approach.

Since different transducers exhibit slight variations in resonant frequency, frequency sweeping is conducted to identify the optimal frequency for each transducer. Fig. 6 illustrates the actual sweep waveforms, with the red waveform representing transducer voltage and the green waveform representing transducer current. The frequency point with the highest current within a specific range is selected as the operating frequency for subsequent operations.

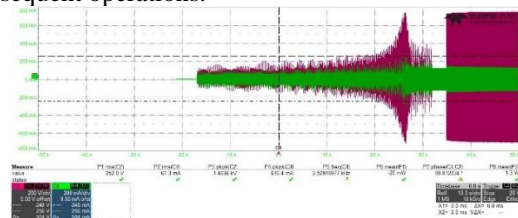


Fig. 6 Frequency Sweep Waveform

Table 1 presents the results of frequency tracking conducted every 3 minutes over a total duration of 9 minutes. The results indicate that the transducer’s power decreases as operating time increases due to a shift in the optimal frequency. However, with frequency tracking,

the transducer returns to its optimal operating point, nearly restoring its initial power level. The transducer's vibration amplitude, illustrated in Fig. 7, decreased by  $9\mu\text{m}$  before tracking but returned to a higher state after tracking, as shown in Fig. 8, demonstrating the effectiveness of the frequency-tracking method. To examine the overall impedance drift, an LCR meter was utilized to compare the transducer's impedance and phase before Fig. 9 and after testing Fig. 10. These figures demonstrate that, following a brief test, the zero-phase frequency shifted from 27.67 kHz to 27.11 kHz. The experimental results indicate that both frequency and vibration amplitude change over time, and frequency tracking effectively mitigates this issue.

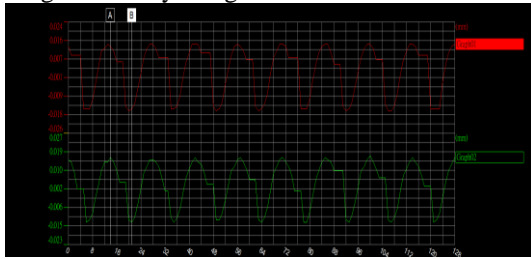


Fig. 7 Vibration Amplitude Before and After Damping

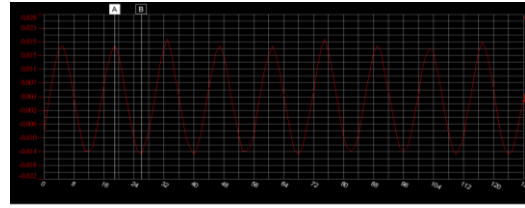


Fig. 8 Vibration Amplitude After Frequency Tracking

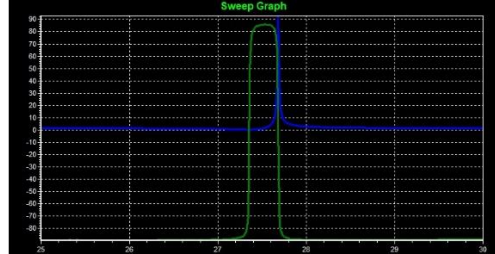


Fig. 9 Before Testing

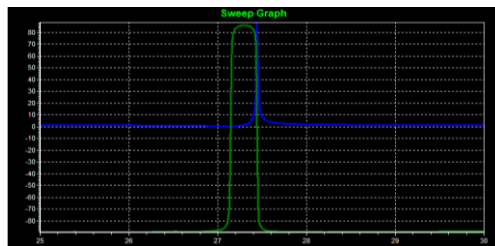


Fig. 10 After Testing

Table 1 Frequency Tracking Results

TIME (min)	V <sub>in</sub> (DC)	L (mH)	C (nF)	f <sub>r</sub> (kHz)	f <sub>s</sub> (kHz)	V <sub>PZ</sub> (V)	I <sub>PZ</sub> (mA)	T <sub>PZ</sub> (°C)	T <sub>L</sub> (°C)	T <sub>water</sub> (°C)	P <sub>in</sub> (W)	P <sub>PZ</sub> (W)
Start	100	3.3	9.4	30.2	27.43	605.0	107.0	27.6	25.3	28.6	44.7	40.4
1					27.42	645.5	115.8	34.1	28.6	41.3	47.0	42.8
3					27.39	588.0	125.9	35.0	28.3	43.7	43.6	39.4
9					27.30	379.0	109.5	39.8	28.7	45.2	29.0	27.6

#### 4. Conclusion

This paper employs a digital frequency sweeping method to identify the optimal frequency point for various transducers under different loads and incorporates a frequency tracking feature. When frequency drift occurs, corrections are made at fixed intervals to maintain a consistent vibration amplitude. Experimental results demonstrate the effectiveness of this method. However, maintaining long-term frequency tracking for system stability is currently not feasible, likely due to factors such as temperature fluctuations, changes in mechanical structure, and the inability of the initially matched LC components to achieve optimal resonance during frequency drift. Future research will focus on addressing these potential issues.

#### 5. References

1. Tsujino, J., Ueoka, T., Hasegawa, K., Fujita, Y., Shiraki, T., Okada, T., & Tamura, T. (1996). New methods of ultrasonic welding of metal and plastic materials. *Ultrasonics*, 34(2-5), 177-185.

2. Li, X., Stritch, T., Manley, K., & Lucas, M. (2021). Limits and opportunities for miniaturizing ultrasonic surgical devices based on a Langevin transducer. *IEEE Transactions on Ultrasonics, Ferroelectrics, and Frequency Control*, 68(7), 2543-2553.
3. I. C. Lien, Y. C. Shu. (2008, Nov). Introduction to Vibration-Base Piezoelectric Energy Harvesting. *Industrial Materials Magazine*.
4. Yang, T., Zhu, Y., Li, S., An, D., Yang, M., & Cao, W. (2020). Dielectric loss and thermal effect in high power piezoelectric systems. *Sensors and Actuators A: Physical*, 303, 111724.
5. DeAngelis, D. A., & Schalcosky, D. C. (2006, October). P2O-10 The Effect of PZT8 Piezoelectric Crystal Aging on Mechanical and Electrical Resonances in Ultrasonic Transducers. In *2006 IEEE Ultrasonics Symposium* (pp. 1935-1938). IEEE.
6. Kazys, R., & Vaskeliene, V. (2021). High temperature ultrasonic transducers: A review. *Sensors*, 21(9), 3200.
7. Piezoelectric Components Business Unit. (2021, March 7). Bolt Clamped Langevin Transducer. <https://www.unictron.com/piezoelectric-components/piezoelectric-technologies/bolt-clamped-langevin-transducer/?lang=zh-hant>

---

---

**Authors Introduction**

**Dr. Chung-Wen Hung**



He received the Ph.D. degrees in Electrical Engineering from National Taiwan University in 2006. Currently he is a Professor in National Yunlin University of Science & Technology. His research interests include the IoT, IIoT, and AI application.

**Mr. Yu-Hsing Su**



He received the B.S. degrees and now he is studying for the M.S. degree in electrical engineering from National Yunlin University of Science and Technology.

**Dr. Chun-Chieh Wang**



He received the PhD degree in The graduate school of engineering science and technology from Nation Yunlin University of Science and Technology. Currently, he is a project professor at National Yunlin University of Science and Technology.